

Are light lead nuclei deformed? Fayans functional *vs* Skyrme–Hartree–Fock functionals

S. V. Tolokonnikov

*Kurchatov Institute, 123182 Moscow, Russia and
Moscow Institute of Physics and Technology, 141700 Dolgoprudny, Russia.*

I. N. Borzov

Joint Institute for Nuclear Research, 141980 Dubna, Russia

M. Kortelainen

*Department of Physics, P.O. Box 35 (YFL), University of Jyväskylä, FI-40014 Jyväskylä, Finland and
Helsinki Institute of Physics, P.O. Box 64, FI-00014 University of Helsinki, Finland*

Yu. S. Lutostansky and E. E. Saperstein

Kurchatov Institute, 123182 Moscow, Russia

First calculations for deformed nuclei with the Fayans functional are carried out for the uranium and lead isotopic chains. We compare our results to Skyrme–Hartree–Fock–Bogolyubov results of HFB-17 and HFB-27 functionals. For the uranium isotopic chain, the Fayans functional predicts results rather similar compared to HFB-17 and HFB-27. However, there is a disagreement for the lead isotopic chain. Both of the Skyrme functionals predict rather strong deformations for the light Pb isotopes. According to our analysis, this contradicts to experimental data on charge radii and magnetic moments of odd the Pb isotopes. The Fayans functional predicts a spherical ground state for all of the lead isotopes, in accordance with the data. Some of the light isotopes, e.g. ^{180}Pb and ^{184}Pb , turned out to be very soft, close to the critical point of the deformation phase transition.

PACS numbers: 21.60.Jz, 21.10.Ky, 21.10.Ft, 21.10.Re

I. INTRODUCTION

A long-standing goal of the low-energy nuclear theory community is to have a unified theoretical framework, applicable to nuclear structure and reactions. Presently, due to computational limitations, the nuclear density functional theory (DFT) is the only microscopical theory which can be applied throughout the entire nuclear chart. In the framework of nuclear DFT, complex many-body correlations are encoded into the energy density functional (EDF), constructed from the nuclear densities and currents. Historically, since the work by Vautherin and Brink [1], the Hartree–Fock (HF) method with the effective Skyrme forces has become very popular in the nuclear physics. From the very beginning, the Skyrme HF method was aimed at calculating global properties of nuclei, such as the binding energy and neutron and proton density distributions. A little later the HF method with the effective Gogny force was suggested [2] and successfully applied to the same objects as the Skyrme HF method. In addition to these, relativistic mean-field (RMF) models have been also employed in the nuclear physics, see Ref. [3] and references therein. In fact, it was quite soon realized that these methods had a rather strong correspondence to DFT methods employed e.g. in atomic physics. Indeed, during the last few decades, mean-field methods in the framework of HF and Hartree–Fock–Bogolyubov (HFB) theory, have been widely used in the nuclear physics [4, 5]. The HFB, a method suit-

able for superfluid nuclei with pairing correlations, is a generalization of the HF, which allows particles and holes to be treated on the equal footing.

The use of density-dependent effective interactions is a common feature of these mean-field approaches. When Skyrme and Gogny effective forces are written as a form of the EDF, a rather simple ansatz for density dependence is assumed. Schematically it reads

$$E_0^{\text{int}}[\rho] = \int \mathcal{E}(\rho(\mathbf{r})) d^3r = \int \frac{a\rho^2}{2} (1 + \alpha\rho^\sigma) d^3r, \quad (1)$$

where $\rho(\mathbf{r})$ is the matter density and a , b , and $\sigma \leq 1$ are parameters. For brevity, we omit for a time the isotopic indices and do not discuss the spin-orbit and other “small” terms of the effective force. As will be later discussed, Fayans functional has more enriched density dependence. Recently, density dependence of Skyrme-like EDFs has been enriched by utilizing density matrix expansion techniques [6–11].

The parameters of Skyrme forces, as well as Gogny and RMF models, have been typically adjusted to the experimental data on nuclear binding energies and charge radii. Many optimization schemes also use data on single-particle levels, fission properties, together with other observables and pseudo-observables. Because data on very neutron rich nuclei is scarce, especially at the time when some of the older Skyrme parameterizations were adjusted, some of the isovector parameters may have larger uncertainties. The best description of nuclear masses

(the root-mean-square deviation from the respective experimental values being smaller than 600 keV) was attained with the HFB-17 EDF in the study of Goriely and his coauthors [12, 13]. This result was achieved, however, by including some phenomenological corrections atop of the mean field.

The Fayans functional [14–18] we use in this work assumes a rather sophisticated density dependence which can be schematically written as

$$\mathcal{E}(\rho) = \frac{a\rho^2}{2} \frac{1 + \alpha\rho^\sigma}{1 + \gamma\rho}. \quad (2)$$

The use of the bare mass, i.e. $m^* = m$, is another peculiarity of the Fayans functional. Both of these features of the Fayans approach are connected to the self-consistent theory of finite Fermi systems (TFFS) [19].

Up to now, all applications of the Fayans functional were limited to spherical nuclei. In addition to the above references, they included the analysis of charge radii [20], of the magnetic [21, 22] and quadrupole [23, 24] moments in odd nuclei, of characteristics of the first 2^+ excitations in even semimagic nuclei [25, 26] and of beta-decay rates [27] as well. Recently, single-particle spectra of magic nuclei were analyzed [28]. In all aforementioned cases, a reasonable description of the data was achieved, better as a rule than in analogous Skyrme HFB calculations.

The aim of this work is to apply for the first time the Fayans functional to deformed nuclei. The principle goal is to study deformation properties of Fayans functional in selected set of isotopic chains. This paves a way for more comprehensive studies with the Fayans functional across the nuclear chart. This article is organized as follows: In Section II, the path from the self-consistent TFFS to the Fayans functional is outlined. In Section III, the version FaNDF⁰ [17] of the Fayans functional is briefly described. Section IV deals with empirical arguments against stable deformations in the ground states of the light lead isotopes. Calculated results for U and Pb isotopes are presented in Section V, and in Section VI we draw our conclusions.

II. SELF-CONSISTENT TFFS AND THE FAYANS FUNCTIONAL

The self-consistent TFFS [19] is based on the general principles of TFFS [29] supplemented with the condition of the self-consistency in the TFFS between the energy-dependent mass operator $\Sigma(\mathbf{r}_1, \mathbf{r}_2; \varepsilon)$, the single-particle Green's function $G(\mathbf{r}_1, \mathbf{r}_2; \varepsilon)$, and the effective NN interaction $\mathcal{U}(\mathbf{r}_1, \mathbf{r}_2, \mathbf{r}_3, \mathbf{r}_4; \varepsilon, \varepsilon')$ [30].

This approach starts from the quasiparticle mass operator $\Sigma_q(\mathbf{r}_1, \mathbf{r}_2; \varepsilon)$ which, by definition [29], coincides with the exact mass operator Σ at the Fermi surface. In the mixed coordinate-momentum representation the operator $\Sigma_q(\mathbf{r}, k^2; \varepsilon)$ depends linearly on the momentum

square k^2 and the energy ε [19, 29],

$$\Sigma_q(\mathbf{r}, k^2; \varepsilon) = \Sigma_0(\mathbf{r}) + \frac{1}{2m\varepsilon_F^0} \mathbf{k} \Sigma_1(\mathbf{r}) \mathbf{k} + \Sigma_2(\mathbf{r}) \frac{\varepsilon}{\varepsilon_F^0}, \quad (3)$$

where $\varepsilon_F^0 = (k_F^0)^2/2m$ is the Fermi energy of nuclear matter, k_F^0 being the corresponding Fermi momentum. By definition, we have

$$\Sigma_1(\mathbf{r}) = \varepsilon_F^0 \left. \frac{\partial \Sigma(\mathbf{r}, k^2; \varepsilon)}{\partial \varepsilon_k} \right|_0, \quad (4)$$

$$\Sigma_2(\mathbf{r}) = \varepsilon_F^0 \left. \frac{\partial \Sigma(\mathbf{r}, k^2; \varepsilon)}{\partial \varepsilon} \right|_0, \quad (5)$$

where $\varepsilon_k = k^2/2m$ and the subscribe “0” means that the energy and momentum variables are taken at the Fermi surface. Thus, the component Σ_2 determines the Z -factor:

$$Z(\mathbf{r}) = (1 - \Sigma_2(\mathbf{r})/\varepsilon_F^0)^{-1}, \quad (6)$$

whereas the inverse effective mass is

$$\frac{m}{m^*(\mathbf{r})} = \frac{(1 + \Sigma_1(\mathbf{r})/\varepsilon_F^0)}{(1 - \Sigma_2(\mathbf{r})/\varepsilon_F^0)}. \quad (7)$$

Usually, the quantity inverse to the numerator is called the “ k -mass”, and the denominator, the “ E -mass”.

The wave functions $\psi_\lambda(\mathbf{r})$ which diagonalize the quasiparticle Green function $G_q = (\varepsilon - \varepsilon_k - \Sigma_q)^{-1}$ obey the following equation

$$\left(\Sigma_0(\mathbf{r}) - \frac{1}{2m\varepsilon_F^0} \nabla \Sigma_1(\mathbf{r}) \nabla + \Sigma_2(\mathbf{r}) \frac{\varepsilon_\lambda}{\varepsilon_F^0} \right) \psi_\lambda = \varepsilon_\lambda \psi_\lambda. \quad (8)$$

They are orthonormalized with the weight,

$$\int d\mathbf{r} \psi_\lambda^*(\mathbf{r}) \psi_{\lambda'}(\mathbf{r}) (1 - \Sigma_2(\mathbf{r})) = \delta_{\lambda\lambda'}. \quad (9)$$

The Lagrange formalism was used in Ref. [19], with the quasiparticle Lagrangian L_q being constructed in such a way that the corresponding Lagrange equations coincide with Eq. (8).

In the double-magic nuclei, which are non-superfluid, the Lagrangian density \mathcal{L}_q , $L_q = \int d\mathbf{r} \mathcal{L}_q(\mathbf{r})$, depends on three sorts of densities $\nu_i(\mathbf{r})$, $i = 0, 1, 2$:

$$\nu_0(\mathbf{r}) = \sum n_\lambda \psi_\lambda^*(\mathbf{r}) \psi_\lambda(\mathbf{r}), \quad (10)$$

$$\nu_1(\mathbf{r}) = -\frac{1}{2m\varepsilon_F^0} \sum n_\lambda \nabla \psi_\lambda^*(\mathbf{r}) \nabla \psi_\lambda(\mathbf{r}), \quad (11)$$

$$\nu_2(\mathbf{r}) = \frac{1}{\varepsilon_F^0} \sum n_\lambda \varepsilon_\lambda \psi_\lambda^*(\mathbf{r}) \psi_\lambda(\mathbf{r}), \quad (12)$$

where ε_λ and n_λ are the quasiparticle energies and occupation numbers, $n_\lambda = (0, 1)$. Evidently, one gets

$$\nu_0(\mathbf{r}) = Z(\mathbf{r})\rho(\mathbf{r}), \quad (13)$$

where the density $\rho(\mathbf{r})$ is normalized to the total particle number. The relation between $\nu_1(\mathbf{r})$ and the Skyrme density $\tau(\mathbf{r})$ is more complicated [19]. The density $\nu_2(\mathbf{r})$ has no analogue in the Skyrme HF theory.

The components Σ_i of the mass operator (3) can be found from the interaction Lagrangian $L'_q[\nu_i]$ as follows:

$$\Sigma_i = \frac{\delta L'_q}{\delta \nu_i}. \quad (14)$$

The simplest ansatz for the quasiparticle Lagrangian which involves the momentum and energy dependence effects on equal footing was suggested in [19]:

$$\mathcal{L}'_q = -C_0 \left(\frac{1}{2} \nu_0 \hat{\lambda}_{00} \nu_0 + \frac{\gamma}{6\rho_0} \nu_0^3 + \hat{\lambda}_{01} \nu_0 \nu_1 + \hat{\lambda}_{02} \nu_0 \nu_2 \right), \quad (15)$$

where $C_0 = (dn/d\varepsilon_F)^{-1} = \pi^2/(p_F m)$ in Eq. (24) is the usual TFFS normalization factor, inverse density of states at the Fermi surface, and $\rho_0 = (k_F^0)^3/3\pi^2$ is the density of one kind of nucleons in equilibrium symmetric nuclear matter. The amplitudes

$$\hat{\lambda}_{ik} = \lambda_{ik} + \lambda'_{ik} \boldsymbol{\tau}_1 \boldsymbol{\tau}_2 \quad (16)$$

are the isotopic matrices and only one of them,

$$\hat{\lambda}_{00}(\mathbf{r}_1, \mathbf{r}_2) = \hat{\lambda}_{00}(1 + \tau_0^2 \Delta_1) \delta(\mathbf{r}_1, \mathbf{r}_2), \quad (17)$$

is the finite range operator. The term proportional to γ , in Eq. (15), results in the density dependence of the main, scalar and isoscalar, Landau–Migdal interaction amplitudes [29].

To minimize the number of new parameters, the ansatz $\lambda'_{01} = \lambda'_{02} = 0$ was used in [19]. In this case, the components Σ_1^T and Σ_2^T of the mass operator do not depend on τ , being the function of the total density $\nu_0^+ = \nu_0^n + \nu_0^p$:

$$\Sigma_1^T(\mathbf{r}) = \frac{\delta L_q}{\delta \nu_1^T(\mathbf{r})} = C_0 \lambda_{01} \nu_0^+(\mathbf{r}), \quad (18)$$

$$\Sigma_2^T(\mathbf{r}) = \frac{\delta L_q}{\delta \nu_2^T(\mathbf{r})} = C_0 \lambda_{02} \nu_0^+(\mathbf{r}). \quad (19)$$

With the use of (13) and (19), one can obtain the explicit dependence of the Z -factor on the density with the usual normalization:

$$Z_\tau(\mathbf{r}) = \frac{2}{1 + \sqrt{1 - 4C_0 \lambda_{02} \rho^+(\mathbf{r})/\varepsilon_F^0}}. \quad (20)$$

The total interaction energy can be found for the Lagrangian (15) according the canonical rules. It corresponds to the following EDF:

$$\mathcal{E}_{\text{int}} = C_0 \left[\frac{1}{2} \hat{\lambda}_{00} (\nu_0^2 - r_p^2 (\nabla \nu_0)^2) + \hat{\lambda}_{01} \nu_0 \nu_1 + \frac{\gamma}{6\rho_0} \nu_0^3 \right]. \quad (21)$$

It does not contain the “new” density ν_2 and converts to the Skyrme EDF at limit $\nu_0 \rightarrow \rho$ and $\nu_1 \rightarrow \tau$. However, the substitution of Eq. (13) with the Z -factor (20) results in rather sophisticated EDF in the self-consistent TFFS, which hardly can be introduced *ad hoc*.

The parameters of the Lagrangian (15) were found in [19] by fitting binding energies, charge radii and single-particle spectra of double-magic nuclei from ^{40}Ca to ^{208}Pb . The found values $\lambda_{01} = 0.31$ and $\lambda_{02} = -0.25$ correspond to the following characteristics of nuclear matter: $m_0^* = 0.95m$ and $Z_0 = 0.8$. The latter agrees with the value found in [31] on the base of the dispersion relation for the quantity $\partial\Sigma/\partial\varepsilon$ [29] in nuclear matter.

In Ref. [14] the so-called Generalized EDF method was formulated as a generalization of the Kohn–Sham (KS) method [32] for superfluid nuclei. In this case, the EDF depends not only on the normal densities $\rho_{n,p}(\mathbf{r})$, but on their anomalous counterparts $\nu_{n,p}(\mathbf{r})$ as well. Independently, similar development of the KS method for suggested in condensed matter physics [33]. The pairing problem was considered in [14] with an elegant method of direct solving Gor'kov equations for spherical systems in the coordinate representation [34]. In practice, this method is close to solving HFB equations which was made firstly in [2] for the Gogny EDF and in [35] for the Skyrme EDF.

The KS method is based on the Hohenberg–Kohn theorem [36] stating that the ground state energy of a Fermi system is a functional of its density. Unfortunately, this theorem does not give any recipe to construct the EDF. Fayans *et al.* [14] found that the EDF (21) can be rather accurately approximated with a rational ρ -dependence of Eq. (2) type. In addition, they used the ansatz $m^* = m$ typical for the KS method. This also agrees with the above estimation. Thus, the Fayans functional can be interpreted as a simplified version of the self-consistent TFFS [19] and the “denominator” in the EDF (2) appears due to the energy dependence effects taken into account in the TFFS.

It is worth to mention that the use of any EDF with density dependence leads to serious problems if one tries to go beyond mean-field multi-reference calculations, such as particle number projection or angular momentum projection [37–40]. Therefore, in this work, we use Fayans functional for single-reference calculations only.

Three sets of the EDF parameters, DF1–DF3, were suggested in Ref. [16], but the most part of calculations with Fayans EDF were carried out with the set DF3 [18] or its version DF3a for transuranium region [41]. Although up to now there are no systematic calculations of nuclear binding energies across the whole nuclear chart within this method, isotopic chains of spherical nuclei were examined in [18, 20, 41]. It was found that the accuracy is only a little worse than that of the best Skyrme HFB calculations. As for the accuracy of reproducing the charge radii [20] of spherical nuclei, typical deviation is of the order of 0.01–0.02 fm, i.e. the agreement is on the

par or higher compared to Skyrme EDF models. This may be linked to more adequate density dependence of the Fayans EDF compared to the Skyrme one. Indeed, if we denote the average error in describing the binding energies as $\overline{\delta E}$ and that for the charge radii as $\overline{\delta R_{\text{ch}}}$, these quantities should be, due to the Hohenberg–Kohn theorem [36], proportional to each other,

$$\overline{\delta R_{\text{ch}}} = \alpha \overline{\delta E}, \quad (22)$$

where the coefficient α depends on the functional we use. As the analysis of [20] showed, for the Fayans EDF this coefficient is less than those of the HFB-17 and SLy4 functionals. Again, this observation may be linked to more enriched density dependence of Fayans functional, which allows to incorporate complex many-body correlations more efficiently. Fayans EDF provides also a high quality description of magnetic [21, 22] and quadrupole [23, 24] moments of odd spherical nuclei, energies and $B(E2)$ values in even semimagic nuclei [25, 26] and beta-decay rates [16, 27]. Recent analysis [28] of the single-particle energies of double-magic nuclei with the Fayans functional *vs* the HFB-17 one also evidences in favor of the first one.

Up to now, all self-consistent calculations with Fayans functionals were carried out for spherical nuclei only. In Ref. [41] deformations for the transuranium nuclei were taken into account approximately. This work presents the first application of Fayans functional to axially deformed nuclei.

III. FANDF⁰ FUNCTIONAL

For completeness, we write down explicitly main ingredients of the Fayans EDF method. In this method, the ground state energy of a nucleus is considered as a functional of normal and anomalous densities,

$$E_0 = \int \mathcal{E}[\rho(\mathbf{r}), \nu(\mathbf{r})] d^3r, \quad (23)$$

where the isotopic indices and the spin-orbit densities are for brevity omitted.

Main distinctions between this method and the Skyrme EDF approach are located in the normal part of the EDF $\mathcal{E}_{\text{norm}}$, containing the central and spin-orbit terms, and Coulomb interaction term for protons. In the major part of applications of this method [15, 16, 18], the DF3 functional was used with the finite range Yukawa-type central force. In this work we use the EDF FaNDF⁰ from [16] with a localized form of the Yukawa function, $Y_u(r) \rightarrow 1 - r_c^2 \nabla^2$, which makes the structure of the surface part of the EDF closer to that of the Skyrme functionals. This form allows us to use a modified version of computer code HFBTHO [42], originally constructed for Skyrme-like EDFs. The parameters of FaNDF⁰ were fitted to the equation of state of nuclear and neutron matter by Friedman and Pandharipande [43] and masses of lead and tin isotopes.

The volume part of the EDF, $\mathcal{E}^v(\rho)$, is taken as a fractional function of densities $\rho_+ = \rho_n + \rho_p$ and $\rho_- = \rho_n - \rho_p$:

$$\mathcal{E}^v(\rho) = C_0 \left[a_+^v \frac{\rho_+^2}{2} f_+^v(x) + a_-^v \frac{\rho_-^2}{2} f_-^v(x) \right], \quad (24)$$

where

$$f_+^v(x) = \frac{1 - h_{1+}^v x^\sigma}{1 + h_{2+}^v x^\sigma} \quad (25)$$

and

$$f_-^v(x) = \frac{1 - h_{1-}^v x}{1 + h_{2-}^v x}. \quad (26)$$

Here, $x = \rho_+/(2\rho_0)$ is the dimensionless nuclear density. The power parameter $\sigma = 1/3$ is chosen in the FaNDF⁰ functional, in contrast to DF3 where $\sigma = 1$ is used. The structure of other terms in the volume parts of these two functionals is kept the same. However, the above mentioned difference leads to significantly different values of the dimensionless parameters in Eqs. (24) – (26) although they still correspond to the same characteristics of nuclear matter, the incompressibility $K_0 = 220$ MeV, equilibrium density $2\rho_0 = 0.16 \text{ fm}^{-3}$ ($r_0 = 1.143$ fm), and energy per particle $\mu = -16.0$ MeV. Parameters denoted by “+” are $a_+^v = -9.559$, $h_{1+}^v = 0.633$, $h_{2+}^v = 1.300$, and parameters denoted by “-” are $a_-^v = 4.428$, $h_{1-}^v = 0.25$, $h_{2-}^v = 1.300$, which all are dimensionless quantities. This parameter set corresponds to the asymmetry energy coefficient of $a_{\text{Sym}} = 30.0$ MeV.

The main difference between FaNDF⁰ and DF3 functionals is in the structure of the surface term. Now it is as follows

$$\mathcal{E}^s(\rho) = C_0 \frac{1}{4} \frac{a_+^s r_0^2 (\nabla \rho_+)^2}{1 + h_{1+}^s x^\sigma + h_{2+}^s r_0^2 (\nabla x_+)^2}, \quad (27)$$

with $h_{1+}^s = h_{2+}^v$, $a_+^s = 0.600$, $h_{2+}^s = 0.440$.

The usual form for the direct Coulomb term of the EDF of Ref. [17] used, the folded charge density ρ_{ch} found with taking into account the proton and neutron form factors. As to the exchange Coulomb term, it was taken as follows

$$- \frac{3}{4} \left(\frac{3}{\pi} \right)^{1/3} e^2 \rho_p^{4/3} (1 - h_{\text{Coul}} x_+^\sigma), \quad (28)$$

with $h_{\text{Coul}} = 0.941$. Such a strong suppression in comparison with the Slater approximation with $h_{\text{Coul}} = 0$ helps to solve the so-called Nollen–Shiffer anomaly [44]. It is worth to mention that similar suppression of the Coulomb exchange term was made in some Skyrme functionals [45].

The usual for the TFFS [29] structure of the spin-orbit term was used in FaNDF⁰ with the same spin-orbit parameters as in the DF3 functional [18].

For completeness, we write down explicitly the anomalous term of the EDF [17],

$$\mathcal{E}_{\text{anom}} = C_0 \sum_{i=n,p} \nu_i^\dagger(\mathbf{r}) f_i^\xi(x_+(\mathbf{r})) \nu_i(\mathbf{r}), \quad (29)$$

where the density dependent dimensionless effective pairing force is

$$f^\xi(x_+) = f_{\text{ex}}^\xi + h^\xi x_+ + f_{\nabla}^\xi r_0^2 (\nabla x_+)^2, \quad (30)$$

with $f_{\text{ex}}^\xi = -2.8$, $h^\xi = 2.8$, $f_{\nabla}^\xi = 2.2$.

All above values of the parameters were found in Ref. [17] by fitting the masses and charge radii of approximately one hundred spherical nuclei from calcium isotopes to lead isotopes.

In our current implementation of the Fayans functional to the computer code HFBTHO, due to technical reasons, we made two small simplifications to the original FaNDF⁰ EDF. Firstly, we used the approximation $\rho_{\text{ch}} = \rho_p$ for the direct Coulomb term. Secondly, we put $f_{\nabla}^\xi = 0$ in (30) making the anomalous EDF closer to that used in [18]. Therefore below we use the above parameters for the normal part of the EDF only. As to the anomalous EDF, the parameters will be found anew and will be given in the corresponding places. As far as we deal with the zero-range pairing force, the strength parameters depend on the cutoff energy E_{cut} in the pairing problem, being also smoothly A dependent [18]. In practice, this means that we take $f^\xi = -0.220$ for U and $f^\xi = -0.224$ for Pb isotopes.

IV. EMPIRICAL ARGUMENTS AGAINST DEFORMATIONS IN THE LIGHT LEAD ISOTOPES

In the point of the phase transition to the deformed state, the charge radius R_{ch} increases sharply, independent on the sign of the quadruple deformation parameter β_2 . This can be easily seen from the Bohr–Mottelson liquid-drop model (LDM) [46] formula for the square of the rms matter radius,

$$\langle r^2 \rangle_{\text{def}} = R_0^2 \left(1 + \frac{5}{4\pi} \sum_L \beta_L^2 \right), \quad (31)$$

where R_0 is the radius of the spherical nucleus and β_L is the dimensionless deformation parameter of L -th multipolarity. In practice, one deals usually with the quadrupole deformation $L = 2$. In the LDM, it is usually assumed that the proton and charge distributions are deformed in the same way as the total nucleon density, hence Eq. (31) can be also applied to the square of charge radius R_{ch}^2 . The second term in the brackets contributes only in the deformed case.

Figure 1 shows the experimental charge radii in lead isotopic chain [47–49], compared to predictions of various theoretical models. As can be seen, HFB-17 and HFB-27 functionals predict a sudden shift in the charge radii, when following down towards light isotopes, failing to reproduce the experimental trend. Contrary to this, the Fayans EDF DF3a [20] agrees well with the experimental data, with an average disagreement of the order of 0.01

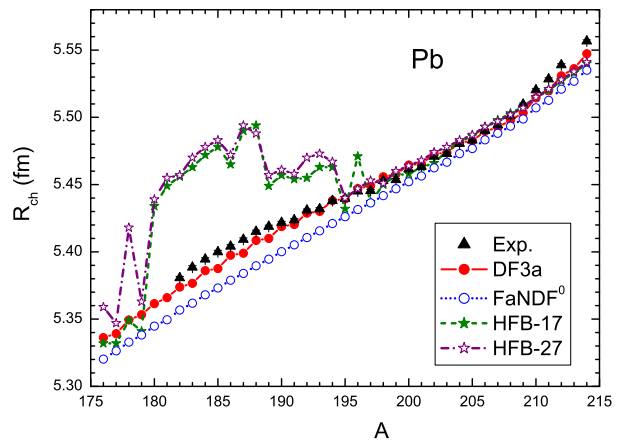


FIG. 1: (Color online) Charge radii of the lead isotopes. Predictions of two Fayans EDFs DF3a and FaNDF⁰ are compared to two Skyrme functionals HFB-17 and HFB-27.

fm. We also show here results for the functional FaNDF⁰ [17], which predicts charge radii close to those of DF3a. For the isotopes heavier than $A = 198$, HFB-17 and HFB-27 results also agree with the experimental trend. Here, appearance of ground-state deformation with both of the HFB functionals is the main contributing reason for this discrepancy. As we will see later, FaNDF⁰ predicts a spherical ground-state for all lead isotopes. The results for DF3a were computed within a spherical symmetry.

Another set of data which, in our opinion, evidences against deformation in the lead isotopic chain are magnetic moments of the odd Pb isotopes, see Fig. 2. The experimental data are taken from [50]. For the spherical form of the even core, the theoretical predictions are taken from [21, 22]. For the $3p_{3/2}$ state they coincide practically with the data, for the $1i_{13/2}$ one, the disagreement is also rather small, of the order of $0.1 \mu_N$, μ_N is the nuclear magneton. If one switches on a stable quadrupole deformation, a gigantic correction to the magnetic moments arises which does not depend on the deformation parameter β_2 .

For $K = I = j$, $K > 1/2$, with the usual for deformed nuclei notation, we have [21, 46]:

$$\mu_{I=j} = (g_R + \mu_j) \frac{j}{j+1}, \quad (32)$$

where g_R is the deformed core gyromagnetic ratio and μ_j , the single-particle magnetic moment. For the latter, that of the spherical nucleus can be used [21], and the solid-body value $g_R = Z/A$, for the gyromagnetic ratio [46]. In the result, we obtain values displayed in Fig. 2. As one can see, if any of considered light Pb isotopes was deformed, we would obtain very strong disagreement with the experimental values of magnetic moments [50]. The deviation is about $0.5 \mu_N$ in the case of the $1i_{13/2}$ state. For the $3p_{3/2}$ state, the disagreement reaches $0.8 \mu_N$.

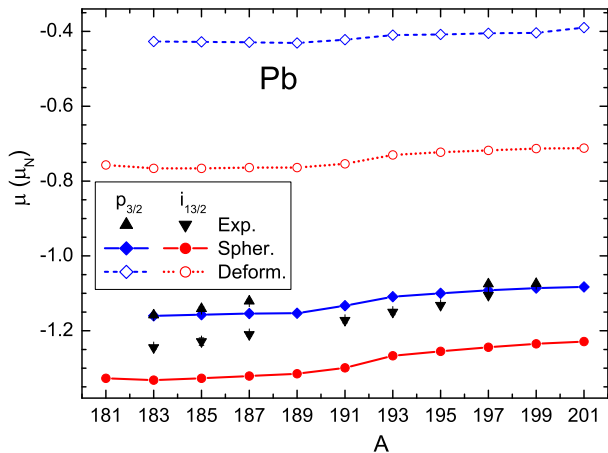


FIG. 2: (Color online) Magnetic moments of odd lead isotopes. Comparison of predictions of the “spherical” calculation [21, 22] based on the DF3 functional with the “deformed” one with the use of Eq. (32).

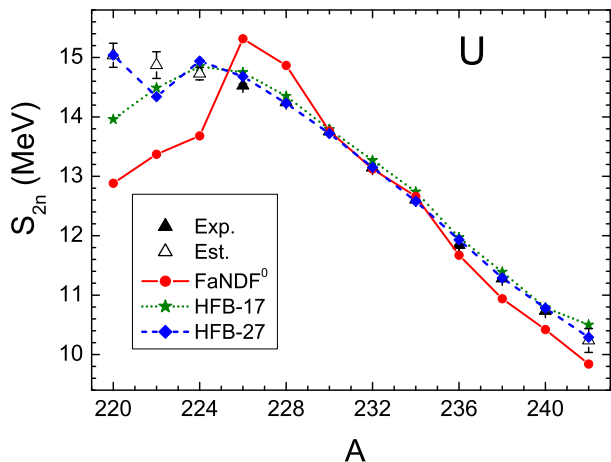


FIG. 3: (Color online) Two-neutron separation energies S_{2n} for even U isotopes. Predictions of the FaNDF⁰ functional are compared to two Skyrme EDFs HFB-17 and HFB-27. Empty triangles show the estimated values [51].

To conclude this section, the experimental data on charge radii of the light lead isotopes as well as on magnetic moments of the odd isotopes do not support an existence of a stable deformation in these nuclei.

V. RESULTS

A. Uranium chain

The aim of this Subsection is to apply the FaNDF⁰ EDF to uranium isotopes which have a well established stable deformation. In this article, due to employed axial computer code, we limit ourselves to the quadrupole deformation β_2 only, with reflection symmetry assumed.

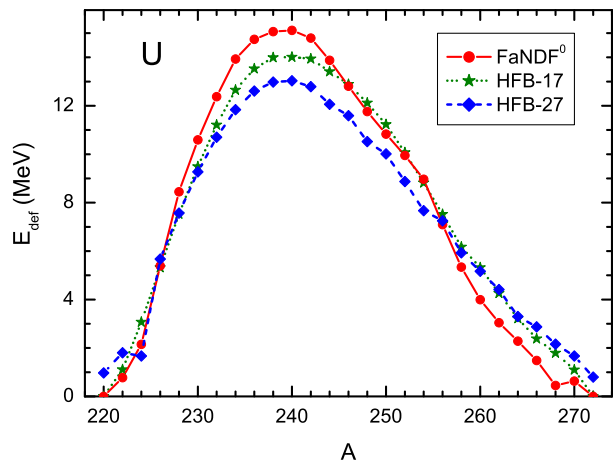


FIG. 4: (Color online) Deformation energy E_{def} for even U isotopes. Predictions of the FaNDF⁰ functional are compared to two Skyrme EDFs HFB-17 and HFB-27.

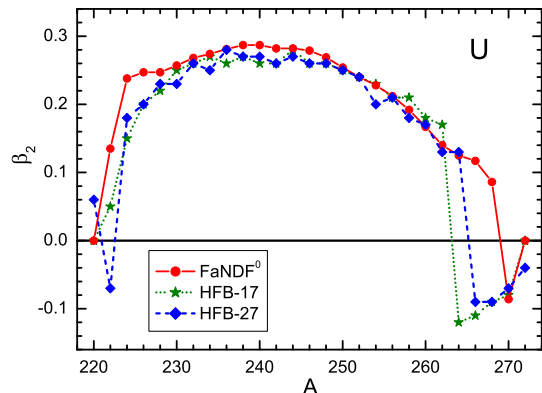


FIG. 5: (Color online) Quadrupole deformation parameter for even U isotopes. Predictions of the FaNDF⁰ functional are compared to two Skyrme EDFs HFB-17 and HFB-27.

The ground states of U isotopes are expected to be axially deformed. Tri-axial deformation usually appears at the top of the fission barriers, not considered in this study. For the uranium chain, we find our results converged when number of the oscillator shells is equal to $N_{\text{sh}} = 25$, i.e. the change of this number to $N_{\text{sh}} = 30$ does not practically influences the results. As to the pairing force, the set of [17] with $f_{\text{ex}}^\xi = -h^\xi$ corresponds to the “surface” pairing with strong attraction at the surface and very small value of f^ξ inside a nucleus. Such model of pairing is typical for all versions of the Fayans functional [18, 25]. Here we found that the deformation energy we are mainly interested for the surface pairing is very close to that for the “volume” pairing model with $h^\xi = 0$, provided the deformation parameter β_2 is less than $0.6 \div 0.8$. To stress the effect of the specific den-

sity dependence of the normal part of the Fayans EDF, we used the simplest one parameter volume pairing. The cutoff energy $E_{\text{cut}} = 60$ MeV is chosen, with corresponding value $f^\xi = -0.220$ fitted to double mass differences for the uranium isotopes.

In Fig. 3, two-neutron separation energies

$$S_{2n}(N, Z) = B(N, Z) - B(N - 2, Z), \quad (33)$$

are shown for uranium isotopes. Comparison is made with experimental data [51] and predictions of the HFB-17 and HFB-27 EDFs. Taking into account that the parameters of the FaNDF⁰ functional were fitted only for spherical nuclei not heavier than the lead, the description of S_{2n} values for uranium isotopes looks rather reasonable. In Figs. 4 and 5, a comparison is presented to the same Skyrme functionals for the deformation energy,

$$E_{\text{def}}(\beta_2) = B(\beta_2) - B(\beta_2 = 0), \quad (34)$$

and the deformation parameter itself. Unfortunately, both of the quantities have no direct experimental equivalent. We see that our calculations with the FaNDF⁰ functional are in reasonable agreement with both the Skyrme EDF predictions. Therefore, it seems reasonable to use this functional for the analysis of the deformation characteristics of the lead isotopes.

B. Lead chain

In the analysis of the lead isotopes, we use the same calculation scheme as for the uranium chain, i.e. $N_{\text{sh}} = 25$ and $E_{\text{cut}} = 60$ MeV is chosen, and the corresponding value $f^\xi = -0.224$ being a bit different. We again begin with the two-neutron separation energies S_{2n} , shown in Fig. 6. On average, agreement with the data is only a little worse than for the HFB-17 and HFB-27 functionals.

As to the deformation characteristics, there is a notable difference between predictions of the Fayans FaNDF⁰ EDF and those of the two Skyrme functionals under consideration. Namely, calculations with the Fayans functional result to a spherical ground state for all of the lead isotopes. At the same time, both of the Skyrme functionals predict a stable deformation in the ground states of many light Pb isotopes. For the HFB-27 functional, deformation appears for isotopes with $A = 170 \div 198$, for the HFB-17 functional, for all isotopes with $A < 204$. For both the functionals, the deformation changes sign from positive for ^{188}Pb to negative for ^{190}Pb , and the deformation is strong for isotopes with $A = 180 \div 192$, $\beta_2 \simeq 0.3$ for $A = 180 \div 188$ and $\beta_2 \simeq -0.2$ for $A = 190 \div 194$ in the case of HFB-27 functional and for $A = 190 \div 196$ in the case of HFB-17 one. Thus, the deformation parameters in this A region are approximately of the same order of magnitude as for U isotopes. The deformation energy is less, $E_{\text{def}} \simeq 3$ MeV, but also is significant. Thus, these predictions of both Skyrme functionals fail to reproduce the experimental trend analyzed in Sect. IV.

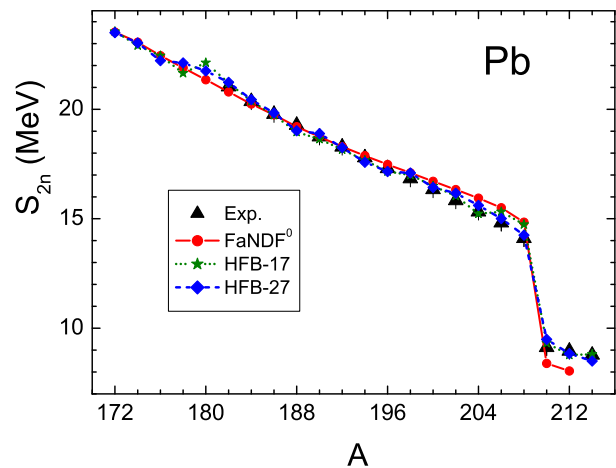


FIG. 6: (Color online) Two-neutron separation energies S_{2n} for even Pb isotopes. Predictions of the FaNDF⁰ functional are compared to two Skyrme EDFs HFB-17 and HFB-27.

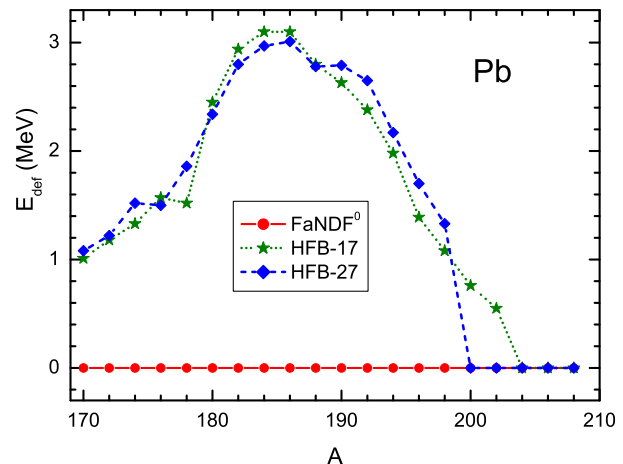


FIG. 7: (Color online) Deformation energy E_{def} for even Pb isotopes. Predictions of the FaNDF⁰ functional are compared to two Skyrme EDFs HFB-17 and HFB-27.

To understand the reason, we calculated the deformation energy curves for different isotopes between ^{172}Pb and ^{216}Pb . As it should be, the magic ^{208}Pb is very rigid. To some extent, this also holds for other heavy and medium isotopes. At the same time, some of lighter isotopes are very soft, e.g. ^{192}Pb and ^{184}Pb nuclei. It seems obvious that some change of the functional could lead to appearance of a stable deformation. This is the case if one goes from the Fayans functional FaNDF⁰ to the Skyrme functionals HFB-17 or HFB-27. The denominator of Eq. (24) may provide some feedback effect preventing the deformation of the light Pb isotopes.

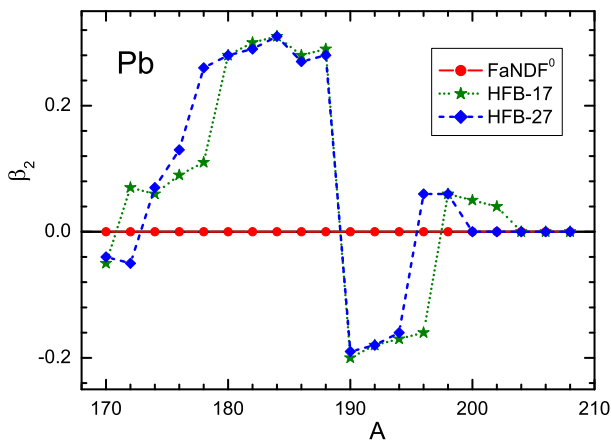


FIG. 8: (Color online) Quadrupole deformation parameter for even Pb isotopes. Predictions of the FaNDF⁰ functional are compared to two Skyrme EDFs HFB-17 and HFB-27.

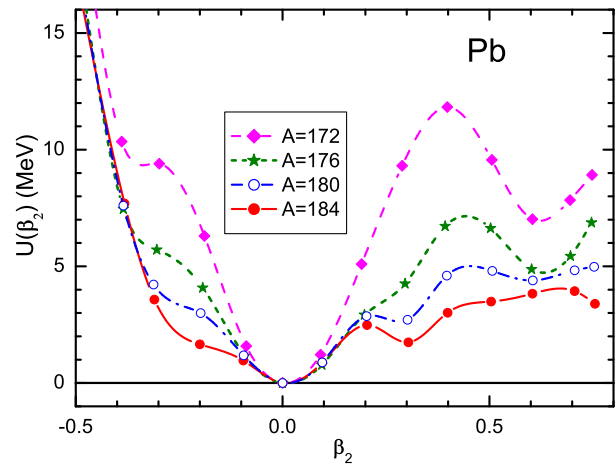


FIG. 11: (Color online) Deformation energy curves $U(\beta_2)$ for light even Pb isotopes.

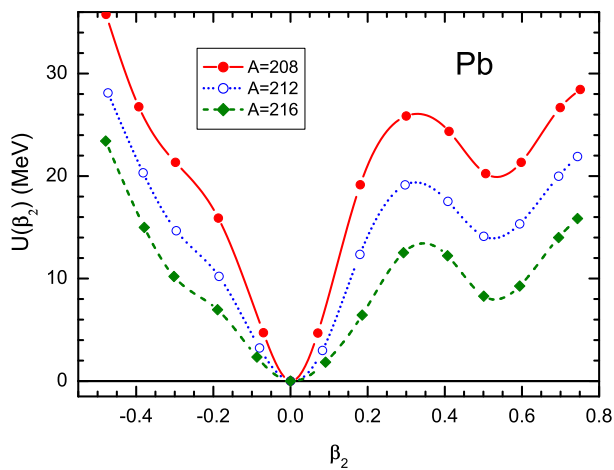


FIG. 9: (Color online) Deformation energy curves $U(\beta_2)$ for heavy even Pb isotopes.

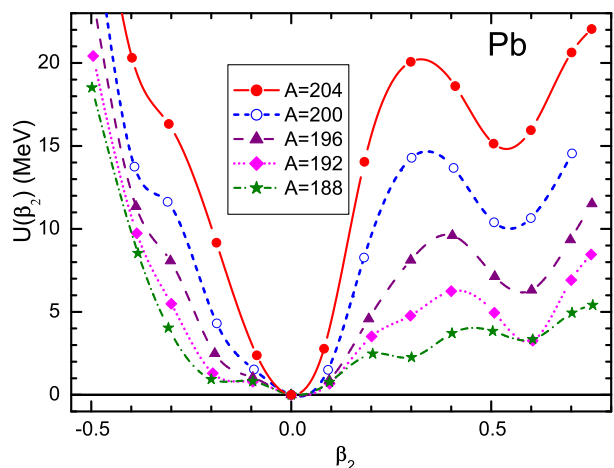


FIG. 10: (Color online) Deformation energy curves $U(\beta_2)$ for medium even Pb isotopes.

VI. CONCLUSION

This article presents the first application of the Fayans functional FaNDF⁰ to deformed nuclei. Fayans functional makes an interesting alternative for Skyrme EDF with some promising properties, as shown in the current work. Comparison was made to two modern Skyrme EDFs: HFB-17 and HFB-27. Results were calculated for the uranium and lead isotopic chains. In the uranium case, our results are qualitatively closer to both, the HFB-17 and HFB-27 functionals. This, however, is not the case for the lead isotopes. Here, both of the HFB functionals predict strong deformation of the light isotopes: $A = 178 \div 196$ for the functional HFB-17 and $A = 178 \div 194$ for the HFB-27. As it is discussed in Section IV, this contradicts to experimental data on the charge radii and magnetic moments. On the contrary, the Fayans functional predicts spherical form for all Pb isotopes, in agreement with experiment. This feature may be linked to a peculiar density dependence of the Fayans functional, resulting from the energy dependence effects of the self-consistent TFFS [19] which are hidden in the formulation in terms of the EDF. A systematic analysis of deformed nuclei with the Fayans functional is necessary to estimate its possible benefits across larger portions of the nuclear chart.

VII. ACKNOWLEDGMENT

The work was partly supported by the Grant NSH-932.2014.2 of the Russian Ministry for Science and Education, and by the RFBR Grants 12-02-00955-a, 13-02-00085-a, 13-02-12106-ofi-m, 14-02-00107-a, the Grant by IN2P3-RFBR under Agreement No. 110291054 and by Swiss National Science Foundation grant no. IZ73Z0_152485 SCOPES.

This work was also supported (M.K.) by Academy of Finland under the Centre of Excellence Programme 2012–2017 (Nuclear and Accelerator Based Physics Pro-

gramme at JYFL) and FIDIPRO programme; and by the European Unions Seventh Framework Programme EN-SAR (THEXO) under Grant No. 262010.

-
- [1] D. Vautherin and D. M. Brink, *Phys. Rev. C* **5**, 626 (1972).
- [2] J. Dechargé and D. Gogny, *Phys. Rev. C* **21**, 1568 (1980).
- [3] P. Ring, *Prog. Part. Nucl. Phys.* **37**, 193 (1996).
- [4] P. Ring and P. Schuck, *The Nuclear Many-Body Problem* (Springer-Verlag, New York, 1980).
- [5] M. Bender, P.-H. Heenen, and P.-G. Reinhard, *Rev. Mod. Phys.* **75**, 121 (2003).
- [6] J. Dobaczewski, B. G. Carlsson, and M. Kortelainen, *J. Phys. G: Nucl. Part. Phys.* **37**, 075106 (2010).
- [7] B. Gebremariam, T. Duguet, and S. K. Bogner, *Phys. Rev. C* **82**, 014305 (2010).
- [8] N. Kaiser, W. Weise, *Nucl. Phys. A* **836**, 256 (2010).
- [9] B. G. Carlsson and J. Dobaczewski, *Phys. Rev. Lett.* **105**, 122501 (2010).
- [10] B. Gebremariam, S. K. Bogner, and T. Duguet, *Nucl. Phys. A* **851**, 17 (2011).
- [11] M. Stoitsov, M. Kortelainen, S. K. Bogner, T. Duguet, R. J. Furnstahl, B. Gebremariam, and N. Schunck, *Phys. Rev. C* **82**, 054307 (2010).
- [12] S. Goriely, N. Chamel, and J. M. Pearson, *Phys. Rev. Lett.* **102**, 152503 (2009).
- [13] S. Goriely, <http://www-astro.ulb.ac.be/bruslib>
- [14] A. V. Smirnov, S. V. Tolokonnikov, and S. A. Fayans, *Sov. J. Nucl. Phys.* **48**, 995 (1988).
- [15] D. J. Horen, G. R. Satchler, S. A. Fayans, and E. L. Trykov, *Nucl. Phys. A* **600**, 193 (1996).
- [16] I. N. Borzov, S. A. Fayans, E. Kromer, D. Zawischa, *Z. Phys. A* **355**, 117 (1996).
- [17] S. A. Fayans, *JETP Letters* **68**, 169 (1998).
- [18] S. A. Fayans, S. V. Tolokonnikov, E. L. Trykov, and D. Zawischa, *Nucl. Phys. A* **676**, 49 (2000).
- [19] V. A. Khodel and E. E. Saperstein, *Phys. Rep.* **92**, 183 (1982).
- [20] E. E. Saperstein and S. V. Tolokonnikov, *Phys. At. Nucl.* **74**, 1277 (2011).
- [21] I. N. Borzov, E. E. Saperstein, and S. V. Tolokonnikov, *Phys. At. Nucl.* **71**, 469 (2008).
- [22] I. N. Borzov, E. E. Saperstein, S. V. Tolokonnikov, G. Neyens, and N. Severijns, *Eur. Phys. J. A* **45**, 159 (2010).
- [23] S. V. Tolokonnikov, S. Kamedzhiev, S. Krewald, E. E. Saperstein, and D. Voitenkov, *EPJA* **48**, 70 (2012).
- [24] S. Kamedzhiev, S. Krewald, S. Tolokonnikov, E. E. Saperstein, and D. Voitenkov. *EPJ Web of Conferences* **38**, 10002 (2012).
- [25] S. V. Tolokonnikov, S. Kamedzhiev, D. Voitenkov, S. Krewald, and E. E. Saperstein, *Phys. Rev. C* **84**, 064324 (2011).
- [26] S. V. Tolokonnikov, S. Kamedzhiev, S. Krewald, E. E. Saperstein and D. Voitenkov. *EPJ Web of Conferences* **38**, 04002 (2012).
- [27] I. N. Borzov, *Nucl. Phys. A* **777**, 645 (2006).
- [28] N. V. Gnezdilov, I. N. Borzov, E. E. Saperstein, and S. V. Tolokonnikov, *Phys. Rev. C* **89**, 034304 (2014).
- [29] A. B. Migdal, *Theory of finite Fermi systems and applications to atomic nuclei* (Nauka, Moscow, 1965; Wiley, New York, 1967).
- [30] S. A. Fayans and V. A. Khodel, *JETP Lett.* **17**, 444 (1973).
- [31] E. E. Saperstein, S. V. Tolokonnikov, *JETP Lett.* **68**, 553 (1998).
- [32] W. Kohn and L. J. Sham, *Phys. Rev.* **140**, A1133 (1965).
- [33] L. N. Oliveira, E. K. U. Gross, and W. Kohn, *Phys. Rev. Lett.* **60**, 2430 (1988).
- [34] S. T. Belyaev, A. V. Smirnov, S. V. Tolokonnikov, S. A. Fayans, *Sov. J. Nucl. Phys.* **45**, 783 (1987).
- [35] J. Dobaczewski, H. Flocard, and J. Treiner, *Nucl. Phys. A* **422**, 103 (1984).
- [36] P. Hohenberg and W. Kohn, *Phys. Rev.* **136**, B864 (1964).
- [37] J. Dobaczewski, M. V. Stoitsov, W. Nazarewicz, and P.-G. Reinhard, *Phys. Rev. C* **76**, 054315 (2007).
- [38] D. Lacroix, T. Duguet, and M. Bender, *Phys. Rev. C* **79**, 044318 (2009).
- [39] M. Bender, T. Duguet, and D. Lacroix, *Phys. Rev. C* **79**, 044319 (2009).
- [40] W. Satuła, J. Dobaczewski, W. Nazarewicz, and M. Rafalski, *Int. J. Mod. Phys. E* **20**, 244 (2011).
- [41] S. V. Tolokonnikov and E. E. Saperstein, *Phys. At. Nucl.* **73**, 1684 (2010).
- [42] M. V. Stoitsov, N. Schunck, M. Kortelainen, N. Michel, H. Nam, E. Olsen, J. Sarich, and S. Wild, *Comp. Phys. Comm.* **184**, 1592 (2013).
- [43] B. Friedman and V. R. Pandharipande, *Nucl. Phys.* **48**, 995 (1988).
- [44] J. A. Nolen, J. P. Schiffer, *Annu. Rev. Nucl. Sci.* **19**, (1969).
- [45] B. A. Brown, *Phys. Rev. C* **58**, 220 (1998).
- [46] A. Bohr and B. R. Mottelson, *Nuclear Structure* (Benjamin, New York, Amsterdam, 1974.), Vol. 2.
- [47] I. Angeli (2008), *Recommended values of nuclear charge radii*, <http://cdfe.sinp.msu.ru/services/radchart/radhelp.html#rad>
- [48] Yu. Gangrsky and K. Marinova (2008), *Nuclear charge radii*, <http://cdfe.sinp.msu.ru/services/radchart/radhelp.html#rad>
- [49] *Database of the Lomonosov Moscow State University, Skobeltsyn Institute of Nuclear Physics*, <http://cdfe.sinp.msu.ru/services/radchart/radmain.html>
- [50] N. J. Stone, *At. Data Nucl. Data Tables* **90**, 75 (2005).
- [51] G. Audi, A. H. Wapstra, and C. Thibault, *Nucl. Phys. A* **729**, 337 (2003).